

# 1 Path independence of climate and carbon cycle response 2 over a broad range of cumulative carbon emissions

3  
4 T. Herrington<sup>1</sup> and K. Zickfeld<sup>1,\*</sup>

5 [1]{Department of Geography, Simon Fraser University, Burnaby, Canada}

6 \*Correspondence to: K. Zickfeld (kzickfel@sfu.ca)

## 7 8 **Abstract**

9 Recent studies have demonstrated the proportional relationship between global warming and  
10 cumulative carbon emissions, yet the robustness of this relationship has not been tested over a  
11 broad range of cumulative emissions and emission rates. This study explores the path  
12 dependence of the climate and carbon cycle response using an Earth System model of  
13 intermediate complexity forced with 24 idealized emissions scenarios across five cumulative  
14 emission groups (1275 GtC - 5275 GtC) with varying rates of emission. We find the century-  
15 scale climate and carbon cycle response after cessation of emissions to be approximately  
16 independent of emission pathway for all cumulative emission levels considered. The ratio of  
17 global mean temperature change to cumulative emissions – referred to as the transient climate  
18 response to cumulative emissions (TCRE) – is found to be constant for cumulative emissions  
19 lower than ~1500 GtC, but to decline with higher cumulative emissions. The TCRE is also  
20 found to decrease with increasing emission rate. The response of Arctic sea ice is found to be  
21 approximately proportional to cumulative emissions, while the response of the Atlantic  
22 meridional overturning circulation does not scale linearly with cumulative emissions, as its  
23 peak response is strongly dependent on emission rate. Ocean carbon uptake weakens with  
24 increasing cumulative emissions, while land carbon uptake displays non-monotonic behavior,  
25 increasing up to a cumulative emission threshold of ~2000 GtC and then declining.

## 26 27 **1 Introduction**

28 Recent studies with coupled climate-carbon cycle models have shown that global mean  
29 temperature change is independent of emission pathway and approximately proportional to

1 cumulative CO<sub>2</sub> emissions (Allen et al. 2009; Matthews et al. 2009; Zickfeld et al. 2009;  
2 Zickfeld et al. 2012; Gillett et al. 2013). Results have also suggested that global mean  
3 temperature remains approximately constant for centuries to millennia after CO<sub>2</sub> emissions  
4 cease (Plattner et al. 2008; Eby et al. 2009; Solomon et al. 2009; Frölicher and Joos 2010;  
5 Gillett et al. 2011; Zickfeld et al. 2013).

6 These studies can be characterized as using the “cumulative emissions framework”, which  
7 relates the instantaneous or century-scale response of global mean temperature to the  
8 cumulative CO<sub>2</sub> emissions over a certain period of time. The ratio of global mean temperature  
9 change to cumulative CO<sub>2</sub> emissions, referred to as the Transient Climate Response to Carbon  
10 Emissions (TCRE), is a measure of both the carbon cycle response to CO<sub>2</sub> emissions and the  
11 physical climate response to atmospheric CO<sub>2</sub> increase, and has been suggested as a useful  
12 benchmark for model intercomparison (Matthews et al. 2009; Gillett et al. 2013). The  
13 cumulative emissions framework is also useful to climate policy discussions for it enables  
14 researchers to express temperature targets, such as the 2°C target adopted by many countries  
15 and international organizations, in terms of a carbon emission “budget” (England et al. 2009;  
16 Meinshausen et al. 2009; Zickfeld et al. 2009; Messner et al. 2010).

17 Several studies explored the robustness of the proportional relationship between the century–  
18 scale and instantaneous global mean temperature change and cumulative emissions. Studies  
19 with both Earth System Models of Intermediate Complexity (EMICs) (Eby et al. 2009;  
20 Zickfeld et al. 2009) and complex Earth System Models (ESMs) (Zickfeld et al. 2012; Nohara  
21 et al. 2013) demonstrated that the *century-scale* temperature response after cessation of  
22 emissions is independent of emissions pathway. Zickfeld et al. (2012), using the Canadian  
23 Earth system model (CanESM), showed that the path independence holds also for a range of  
24 other climate variables (atmospheric CO<sub>2</sub> concentration, precipitation, sea ice cover, Atlantic  
25 meridional overturning circulation). Nohara et al. (2013) obtained similar results with the  
26 Community Earth System Model (CESM), except for the response of the Atlantic meridional  
27 overturning circulation, which was found to exhibit path dependence in a cumulative CO<sub>2</sub>  
28 emission overshoot scenario.

29 A range of studies also explored the robustness of the proportional relationship between the  
30 *instantaneous* global mean temperature change and cumulative emissions by evaluating the  
31 constancy of the TCRE. Matthews et al. (2009), using results from C<sup>4</sup>MIP simulations found  
32 the TCRE to be constant up to cumulative emissions of about 2000 GtC. This result was

1 confirmed by Gillett et al. (2013), who used results from the CMIP5 1% CO<sub>2</sub> increase  
2 experiment. Both studies tested the constancy of the TCRE for one emission scenario only.  
3 Zickfeld et al. (2012) explored the TCRE for a set of scenarios with varying emission rates,  
4 and found it to be approximately constant across scenarios. Krasting et al. (2014), on the other  
5 hand, using a range of scenarios with constant CO<sub>2</sub> emission rates (2 - 25 GtC yr<sup>-1</sup>), found the  
6 TCRE to vary with emission rate. They found the TCRE to be highest at low and high  
7 emission rates, and lowest at present-day emission rates (5 - 10 GtC yr<sup>-1</sup>).

8 Previous studies exploring the proportional relationship between climate change and  
9 cumulative carbon emissions either focused on a single emission scenario (Matthews et al.  
10 2009; Gillett et al. 2013) or on emission scenarios with cumulative CO<sub>2</sub> emissions of up to  
11 about 2500 GtC (Zickfeld et al. 2012; Nohara et al. 2013). Here we use the University of  
12 Victoria Earth System Climate Model (UVic ESCM) to explore the transient climate and  
13 carbon cycle response to emission pathways spanning a broad range of cumulative CO<sub>2</sub>  
14 emissions and CO<sub>2</sub> emission rates. To this scope, we design a set of CO<sub>2</sub> emission scenarios  
15 pertaining to five cumulative emission groups (1275 GtC, 2275 GtC, 3275 GtC, 4275 GtC,  
16 and 5275 GtC). Each cumulative emission group includes a variety of peak-and-decline  
17 scenarios, an “overshoot” scenario entailing negative CO<sub>2</sub> emissions, and a “pulse” scenario  
18 with instantaneous CO<sub>2</sub> release.

19 The paper begins with an overview of the UVic ESCM, followed by a description of the  
20 emission scenarios designed for the purpose of this study. The Results/Discussion section is  
21 divided into three main components. First, the transient response of the physical climate  
22 system is explored. Next, an analysis of the relationship between physical climate variables  
23 and cumulative emissions is presented, followed by an exploration of the carbon cycle  
24 response. Finally, the paper ends with a summary of key findings and conclusions.

25

## 26 **2 Methods**

### 27 **2.1 Model description**

28 The study utilized the UVic ESCM version 2.9, which includes an ocean general circulation  
29 model coupled to a sea ice model and energy-moisture balance model of the atmosphere, and  
30 land and ocean carbon cycle models. The ocean model consists of a primitive 3-dimensional,  
31 19-layer ocean general circulation model with isopycnal mixing and a Gent and McWilliams

1 (1990) parameterization of the effect of eddy-induced tracer transport. Diapycnal mixing is  
2 modeled using a horizontally constant profile of diffusivity with values on the order of  
3  $0.3 \times 10^{-4} \text{ m}^2 \text{ s}^{-1}$  in the pycnocline (Weaver et al. 2001; Eby et al. 2009). Coupled to the ocean  
4 model are a dynamic-thermodynamic sea ice model, and a thermodynamic energy-moisture  
5 balance model of the atmosphere with dynamical feedbacks (Weaver et al. 2001). Land  
6 surface and terrestrial vegetation dynamics are modeled using a simplified version of the  
7 Hadley Centre Met Office surface exchange scheme (MOSES) coupled to the Top-Down  
8 Representation of Interactive Foliage and Flora Including Dynamic vegetation model  
9 (TRIFFID) (Meissner et al. 2003). Ocean carbon is represented via an Ocean Carbon Cycle  
10 Model Intercomparison Project (OCMIP) type inorganic ocean carbon cycle model and a  
11 nutrient-phytoplankton-zooplankton-detritus marine ecosystem model (Schmittner et al.  
12 2005). Sediment processes are represented using an oxic-only model of sediment respiration  
13 (Archer 1996). Model coverage is global with a zonal resolution of  $3.6^\circ$  and meridional  
14 resolution of  $1.8^\circ$  (Weaver et al. 2001).

## 15 **2.2 Model simulations**

### 16 **2.2.1 Historical simulation**

17 The historical simulation was started from the model's pre-industrial (year-1800) control  
18 configuration (with a  $\text{CO}_2$  concentration of 284 ppm), and integrated to the year 2008 using  
19 the observed  $\text{CO}_2$  fossil fuel (Boden et al. 2012) emissions, along with radiative forcing from  
20 non- $\text{CO}_2$  greenhouse gas ( $\text{CH}_4$ ,  $\text{N}_2\text{O}$ , and halocarbons) and sulphate aerosols. The model was  
21 also forced with historical land-cover changes. Since  $\text{CO}_2$  emissions from land-use change  
22 (LUC) generated by the UVic ESCM are small, these emissions were complemented by  
23 externally prescribed LUC emissions to match the observations-based estimate of Houghton  
24 (2008). Natural forcings, including solar variations (due to changes in solar luminosity and  
25 orbital configuration) and volcanic eruptions, were applied using the observed forcing until  
26 2000, and then kept at constant 2000-levels over the rest of the simulation. Between 1800 and  
27 2008, the cumulative  $\text{CO}_2$  fossil fuel and LUC emissions were 347 GtC and 227 GtC,  
28 respectively, resulting in a year 2008  $\text{CO}_2$  concentration of 382 ppm.

## 1 **2.2.2 Future emission pathways**

2 Twenty four idealized emission scenarios across five cumulative emission groups (1275 GtC,  
3 2275 GtC, 3275 GtC, 4275 GtC, and 5275 GtC) were designed (Table 1). These scenarios  
4 include both fossil fuel and land use change emission, and span a variety of peak and decline  
5 scenarios with varying emission rates, as well as cumulative emission “overshoot” scenarios  
6 with negative emissions and instantaneous pulse scenarios (Figure 1). The emission scenarios  
7 were designed by setting a target peak emission rate and a target year of emission cessation,  
8 and ensuring total cumulative emissions (from 1800 onwards) fit into one of the five  
9 aforementioned cumulative emission groups. The emission scenarios include a cumulative  
10 1000–5000 GtC of fossil fuel emissions as well as a cumulative 275 GtC of externally  
11 prescribed LUC emissions. Prescribed LUC emissions follow the historical LUC emissions to  
12 2008 and then decline linearly, reaching zero by 2100. In addition, the emission scenarios  
13 include ~50 GtC of internally calculated LUC emissions from imposed land use changes.  
14 Note that scenarios are labeled according to the total externally prescribed fossil fuel and  
15 LUC emissions (1275 GtC, 2275 GtC, 3275 GtC, 4275 GtC, and 5275 GtC)

16 Emission scenarios were used to force future simulations spanning the period 2008-3000.  
17 Simulations were run with the same forcings as over the historical period. Land use and solar,  
18 orbital, and volcanic radiative forcings were kept constant at year 2000-levels, while sulphate  
19 and non-CO<sub>2</sub> GHGs followed the Special Report on Emission Scenarios (SRES) A2 scenario  
20 until 2010, and were held constant at year 2010 levels thereafter.

21

## 22 **3 Results and discussion**

### 23 **3.1 Physical climate changes**

#### 24 **3.1.1 Atmospheric CO<sub>2</sub> concentration**

25 Peak atmospheric CO<sub>2</sub> concentration varies from 575ppm in the 1275 GtC VFAST scenario  
26 to 2521 ppm in the 5275 GtC PULSE scenario (Figure 2). Scenarios with higher emission  
27 rates yield higher peak CO<sub>2</sub> concentrations; a function of land and ocean carbon sinks being  
28 unable to keep up with faster emission rates (Eby et al. 2009; Zickfeld et al. 2012).

29 Though the short-term CO<sub>2</sub> concentration varies by scenario, the CO<sub>2</sub> concentration begins to  
30 converge after emission cessation for scenarios with the same cumulative emissions, and the

1 long-term CO<sub>2</sub> concentration (by the year 3000) is independent of the emissions rate; a  
2 characteristic which is common to all five cumulative emission groups.

3 Initially, the increased atmospheric CO<sub>2</sub> concentration promotes increased photosynthesis and  
4 water use efficiency in plants (“CO<sub>2</sub> fertilization”; Wullschleger et al. 2002) allowing for  
5 rapid uptake of CO<sub>2</sub> by the land. However, as emissions cease and CO<sub>2</sub> declines while surface  
6 air temperature remains elevated, the land becomes a weak net carbon source, leaving the  
7 much slower ocean sink to take up excess CO<sub>2</sub> (Figure 9).

### 8 **3.1.2 Surface air temperature**

9 The short-term response of global mean surface air temperature (SAT) is dependent on  
10 emission scenario, with scenarios entailing higher maximum emission rates yielding a faster  
11 initial increase in temperature (Figure 3). After emissions cease, however, temperature curves  
12 within a cumulative emissions group converge towards a common value, suggesting that the  
13 long-term (year 3000) global mean temperature response is pathway independent and only  
14 dependent on the overall cumulative emissions (Eby et al. 2009; Zickfeld et al. 2009; Zickfeld  
15 2012). Remarkably, despite substantially higher peak CO<sub>2</sub> concentrations in the OVST and  
16 PULSE scenarios, the peak temperature is nearly identical to that of the other scenarios in the  
17 same cumulative emissions group, suggesting that the peak temperature anomaly is also  
18 approximately independent of the emission rate (Allen et al. 2009). The year-3000 global  
19 mean temperature anomaly (relative to the year 1800) ranges between 2.4°C for the 1275 GtC  
20 scenarios and 8.9°C for the 5275 GtC scenarios. The spatial pattern of temperature change at  
21 the year 3000 is shown in Figure 4 for one select scenario from each cumulative emission  
22 group.

23 The temperature anomaly after cessation of emissions is found to remain approximately  
24 constant, with lower cumulative emission groups (1275 and 2275 GtC) showing a slight  
25 temperature decline after peaking, and higher cumulative emission groups (3275 – 5275 GtC)  
26 showing a slight temperature increase. The near-constancy of global mean temperature after  
27 cessation of emissions is in agreement with earlier modeling studies (Matthews et al. 2008;  
28 Plattner et al. 2008; Eby et al. 2009; Solomon et al. 2009; Lowe et al. 2009; Frölicher and  
29 Joos 2010; Gillett et al. 2011; Zickfeld et al. 2012) and is thought to arise because the cooling  
30 effect associated with declining CO<sub>2</sub> is compensated by reduced ocean heat uptake (Eby et al.  
31 2009).

1 A study by Frölicher et al. (2014) tested an instantaneous pulse scenario with cumulative  
2 carbon emissions of 1800 GtC and found that surface air temperature increases for several  
3 centuries after an initial decrease following emission cessation. They suggest that this is due  
4 to the warming associated with a decrease in ocean heat uptake together with feedback effects  
5 arising in response to the geographic structure of ocean heat uptake overcompensating the  
6 cooling associated with a decline in radiative forcing. In our simulations, surface air  
7 temperature decreases following emission cessation for cumulative emissions in the range  
8 1275-2275 GtC and increases for cumulative emissions of 4275-5275 GtC. The reason for the  
9 slight continued increase in temperature following emission cessation in the larger cumulative  
10 emission groups in our study is that the climate system takes longer to equilibrate with the  
11 radiative forcing, i.e. the decline in ocean heat uptake is smaller, leading to larger warming.

12 We also found the *regional* temperature response at the year 3000 to be approximately  
13 independent of emission pathway. For instance, the maximum temperature difference between  
14 the 5275 GtC PULSE and SLOW scenarios at the year 3000 is  $\sim 0.2^{\circ}\text{C}$  over Central Asia  
15 (Figure 4, panel F).

### 16 **3.1.3 Thermosteric sea level**

17 Global thermosteric sea level rise, defined as the rise in sea level due to thermal expansion of  
18 the ocean, is much slower to react to the increased radiative forcing than surface temperature.  
19 The year 3000 thermosteric sea level rise (relative to 1800) ranges between 0.9 m for the 1275  
20 GtC scenarios to 2.7 m for the 5275 GtC PULSE scenario (Figure 5). Though thermosteric  
21 sea level rise shows sensitivity to the emission rate for centuries after emissions cease (with  
22 faster emission rates yielding a faster initial sea level rise), the curves slowly converge over  
23 the course of the simulation, such that even in the 5275 GtC simulations, there is only a 0.08  
24 m difference between the SLOW and PULSE simulations by the year 3000.

25 The finding of path dependence of thermosteric sea level rise on century timescales is similar  
26 to the finding of Zickfeld et al. (2012) and Bouttes et al. (2013) and results from the  
27 proportionality of thermosteric sea level rise to the time integrated radiative forcing on those  
28 timescales (Bouttes et al. 2013). Convergence of the sea level response at the end of the 1200-  
29 year long simulation for all cumulative emission groups, however, indicates that on longer  
30 timescales sea level rise is determined primarily by cumulative emissions.

### 1 **3.1.4 Arctic sea ice**

2 September Arctic sea ice disappears completely in the 3275-5275 GtC scenarios, while it  
3 reaches a minimum of about  $0.25 \times 10^6$  to  $0.28 \times 10^6$  km<sup>2</sup> (~5.5 to 6% of the year 2000 value)  
4 in the 2275 GtC scenarios, and  $2.6 \times 10^6$  km<sup>2</sup> in the 1275 GtC scenarios (~58 % of the year  
5 2000 value) (Figure 6).

6 The rate of sea ice decline is path dependent, and a function of the CO<sub>2</sub> emission rate.  
7 Emission scenarios with a higher maximum CO<sub>2</sub> emission rate display the fastest declines.  
8 The minimum sea ice extent, on the other hand, is independent of emission pathway.

9 Our simulations suggest that there is a threshold cumulative emissions level at which the  
10 modeled climate is no longer able to support year-round sea ice cover. Using the definition of  
11 an ice-free Arctic adopted by the IPCC's Fourth Assessment Report (AR4), in which a  
12 minimum ice extent of  $\leq 1.0 \times 10^6$  km is considered ice free (Solomon et al. 2007), this  
13 threshold lies between 1275 and 2275 GtC.

14 The UVic model fails to capture the current observed trends of rapid ice loss in the last  
15 decade (Comiso 2012), a problem that plagues many climate models (Stroeve et al. 2007).  
16 The inability of the model to simulate the observed decline in sea ice suggests that the  
17 threshold cumulative emission levels for an ice-free Arctic in the summer may be lower than  
18 indicated by this study.

### 19 **3.1.5 Atlantic Meridional overturning circulation**

20 The modeled Atlantic Meridional Overturning Circulation (AMOC) index (defined as the  
21 maximum of the overturning streamfunction) is 20.7 Sv in the year 2000, which is in  
22 relatively good agreement with observations (~12 to ~30 Sv over the past decade) (Send et al.  
23 2011). The simulated AMOC is quite robust for even in the 5275 GtC scenarios the AMOC  
24 index never falls below 13 Sv or ~59% of the preindustrial value before recovering (Figure 7).  
25 Recovery of the AMOC occurs after temperatures at high latitudes begin to stabilize and  
26 freshwater fluxes into the North Atlantic begin to stabilize or slow, allowing the overturning  
27 circulation to export some of the excess freshwater from the region.

28 The transient response of the AMOC is dependent on emission pathway – with pathways  
29 displaying higher emission rates producing a faster decline and a deeper minimum. The long-



1 term (year 3000) response of the AMOC, however, is path independent, although the curves  
2 are slower to converge at higher cumulative emission levels.

3 Rahmstorf (2000) suggested that the AMOC may be subject to hysteresis or multiple stable  
4 states – where the overturning circulation can be on or off, or associated with different  
5 locations of deep water formation. The robustness of the AMOC in the UVic model, even at  
6 extremely high CO<sub>2</sub> concentrations (such as in the case of the 5275 GtC scenarios), either  
7 suggests that multiple stability states are not present in the UVic ESCM, or that the forcing is  
8 below the critical threshold required to induce a state transition. The model, however, does  
9 not include all potential feedbacks on the AMOC, including those associated with melt-water  
10 fluxes from Greenland, so it is possible that the AMOC decline is underestimated by the  
11 model.

## 12 **3.2 Relationship between physical climate response and cumulative** 13 **emissions**

### 14 **3.2.1 Surface air temperature**

15 Consistent with previous studies (Matthews et al. 2009; Zickfeld et al. 2012; Gillett et al.  
16 2013), we find an approximately linear relationship between the modeled instantaneous  
17 surface air temperature change ( $\Delta T$ ) and total cumulative emissions ( $E_c$ ) (Fig. 9, Panel A). We  
18 use linear regression to calculate the ratio of  $\Delta T$  to  $E_c$ , referred to as the Transient Climate  
19 Response to Cumulative Emissions (TCRE) (Gillett et al. 2013). We obtain values of 1.9°C to  
20 2.0°C per trillion tons of carbon (TtC) for the 1275 GtC scenarios, 1.8°C-1.9°C TtC<sup>-1</sup> for the  
21 2275 GtC scenarios, 1.6°C–1.7°C TtC<sup>-1</sup> for the 3275 GtC scenarios, 1.5°C–1.6°C TtC<sup>-1</sup> for the  
22 4275 GtC scenarios, and 1.3-1.5°C TtC<sup>-1</sup> for the 5275 GtC scenarios. These results indicate  
23 that the TCRE decreases with increasing cumulative emissions. Furthermore, the slight  
24 variation of the TCRE within cumulative emission groups suggests that the TCRE is sensitive  
25 to the emission rate, with the TCRE decreasing with increasing rates of emission. The TCRE  
26 calculated at the time of doubling of the pre-industrial CO<sub>2</sub> concentration ranges between  
27 1.7°C TtC<sup>-1</sup> (for the 5275 GtC OVST scenario) and 1.9°C TtC<sup>-1</sup> (for the 1275 GtC scenarios).

28 The spread in the regression-based TCRE values of 0.6°C TtC<sup>-1</sup> for the scenarios examined in  
29 this study compares to a spread of 1.1°C TtC<sup>-1</sup> for C<sup>4</sup>MIP models (1.0°C – 2.1°C TtC<sup>-1</sup>;  
30 Matthews et al. 2009) and 1.6°C TtC<sup>-1</sup> for CMIP5 models (0.8°C – 2.4°C TtC<sup>-1</sup>; Gillett et al.  
31 2013). This indicates that the sensitivity of the TCRE to emission pathway is substantial,

1 albeit smaller than the sensitivity to structural differences in the suite of C<sup>4</sup>MIP and CMIP5  
2 models.

3 The tendency for the TCRE to decrease at higher cumulative emissions was noted in earlier  
4 studies for cumulative emissions in excess of 2000 GtC (Matthews et al., 2009) and 3000 GtC  
5 (Gillett et al. 2013). The linear relationship between  $\Delta T$  and  $E_c$  depends on the cancellation of  
6 the saturation of carbon sinks with increasing  $E_c$  (which results in a larger airborne fraction;  
7 see Figure 9) and the logarithmic dependence of radiative forcing on atmospheric CO<sub>2</sub> (which  
8 results in a smaller increase in radiative forcing per unit CO<sub>2</sub> increase at higher CO<sub>2</sub> levels).  
9 The decrease in TCRE with increasing  $E_c$  suggests that the effect of saturation of the radiative  
10 forcing dominates over the effect of a higher airborne fraction of CO<sub>2</sub> at higher cumulative  
11 emissions in the UVic ESCM.

12 In a study with the GFDL model using scenarios with a range of linear emission increase  
13 rates, Krasting et al. (2014) found the TCRE to increase with increasing emission rates (for  
14 emission rates of 5-25 GtC yr<sup>-1</sup>), which is the opposite tendency from that found in this study.  
15 The TCRE is determined by the effect of the CO<sub>2</sub> emission rate on carbon and ocean heat  
16 uptake (Krasting et al, 2014): a higher CO<sub>2</sub> emission rate results in a larger airborne fraction  
17 and hence higher atmospheric CO<sub>2</sub> levels and radiative forcing. On the other hand, the climate  
18 system is less equilibrated with the radiative forcing, such that a lower fraction of the  
19 equilibrium warming is realized compared to scenarios with slower emission rates. Whether  
20 the TCRE increases or decrease with higher emission rates depends on the balance between  
21 these two processes. Ocean heat and carbon uptake are determined by ocean mixing, and the  
22 equilibration timescale is a function of equilibrium climate sensitivity, quantities that differ  
23 widely among models. It is therefore conceivable that such differences cause the opposite  
24 dependence of TCRE on emission rate in our study compared to that of Krasting et al. (2014).

25 The version of the UVic ESCM used for this study does not include a permafrost carbon  
26 model. Consideration of permafrost carbon would affect the magnitude of warming and could  
27 potentially affect the linear relationship between warming and cumulative carbon emissions.  
28 As the permafrost thaw depth would increase with warming, it would expose more carbon to  
29 decomposition, driving further carbon release – a process known as permafrost carbon  
30 feedback (MacDougall et al. 2012). This feedback could affect the airborne fraction and hence  
31 the approximate constancy of the TCRE. McDougall (2014) shows that inclusion of the  
32 permafrost carbon feedback enhances the sensitivity of the TCRE to the rate of CO<sub>2</sub>

1 emissions, with the TCRE declining more strongly with increasing rate of emissions. Overall,  
2 however, the permafrost carbon feedback does not appear to compromise the approximately  
3 linear relationship between global warming and cumulative carbon emissions (McDougall,  
4 2014).

### 5 **3.2.2 Peak temperature**

6 The relationship between peak surface air temperature and cumulative emissions (Allen et al.  
7 2009) shows a slight deviation from linearity as cumulative emissions increase (Figure 8,  
8 Panel B). Within cumulative emissions groups, the peak temperature is approximately  
9 independent of the emissions rate, with the exception of the 1275 and 2275 GtC OVST  
10 scenarios. The peak at higher cumulative emissions in the 1275 and 2275 GtC OVST  
11 scenarios is the result of the fact that in these scenarios, peak temperature occurs during the  
12 overshoot phase, whereas in the higher cumulative emission groups, peak temperature occurs  
13 near the end of the millennium.

### 14 **3.2.3 Atlantic Meridional overturning circulation**

15 The peak response of the AMOC is dependent on the emission pathway, with scenarios  
16 entailing the highest emission rates yielding the largest declines in overturning circulation.  
17 The minimum overturning, unlike peak surface air temperature, does not display a linear  
18 relationship with cumulative emissions (Figure 8, Panel C). The minimum overturning shows  
19 strong path dependence with higher emission rates yielding a deeper AMOC minimum. We  
20 also find that the minimum overturning decreases with increasing cumulative emissions.

21 The instantaneous AMOC response does not scale well with cumulative emissions either (not  
22 shown), consistent with the result from earlier studies (Zickfeld et al. 2012; Nohara et al.  
23 2013).

### 24 **3.2.4 Arctic sea ice**

25 Similar to the findings of Zickfeld et al. (2012), the response of September Arctic sea ice ( $\Delta I$ ),  
26 which is closely correlated to Northern Hemisphere temperature change, scales approximately  
27 linearly with cumulative emissions. There generally is, however, a steeper change in sea ice  
28 per unit change in cumulative emissions ( $\Delta I/E_c$ ) for scenarios with lower rates of emission  
29 and lower cumulative emissions (Figure 8, Panel D). This likely arises from the fact that the  
30 TCRE declines with increasing cumulative emissions and increasing emission rates.

## 1 **3.3 Changes in the carbon cycle**

### 2 **3.3.1 Atmospheric carbon burden**

3 Until emissions cease, the airborne fraction (defined as the ratio of atmospheric carbon burden  
4 changes to cumulative emissions) varies substantially across emission pathways within the  
5 same cumulative emission group (Figure 9, Panels A and B), and is largest for emission  
6 pathways with the highest emission rates. For the 5275 GtC scenarios, the maximum airborne  
7 fraction varies between 72% for the SLOW scenario and 90% for the PULSE scenario.

8 The airborne fraction also varies substantially between cumulative emissions groups,  
9 increasing with increasing cumulative emissions, similar to Plattner et al. 2008 and Zickfeld et  
10 al. 2013. For the lower cumulative emission groups (1275 and 2275 GtC), less than half of the  
11 emitted CO<sub>2</sub> remains airborne by the year 3000, while for higher cumulative emission groups,  
12 more than half of the emitted CO<sub>2</sub> still resides in the atmosphere. The year-3000 airborne  
13 fraction is 29% for the 1275 GtC scenarios and 63% for the 5275 GtC scenarios.

### 14 **3.3.2 Ocean Carbon Uptake**

15 The ocean takes up a large proportion of the cumulative emissions (Figure 9, Panels E and F).  
16 Until emission cessation, ocean carbon uptake is relatively rapid, with >50% of the emissions  
17 taken up before emissions cease. Uptake slows substantially afterwards, primarily due to  
18 declining atmospheric CO<sub>2</sub> levels.

19 The ocean uptake fraction decreases significantly with increasing cumulative emissions. By  
20 the year 3000, ocean carbon uptake amounts to 56% of cumulative emissions in the 1275 GtC  
21 scenarios, and 35% in the 5275 GtC scenarios. The decrease in ocean uptake fraction with  
22 increasing cumulative emissions is due to a decrease in the CO<sub>2</sub> buffering capacity of the  
23 ocean and stronger climate-carbon cycle feedbacks at higher cumulative emissions (Plattner et  
24 al. 2008; Zickfeld et al. 2013).

25 Ocean carbon uptake across the different emission scenarios is slower to converge than for  
26 atmospheric CO<sub>2</sub> – a function of the ocean's sluggish response to changes in atmospheric  
27 forcing. By the year 3000, however, the differences across scenarios within a cumulative  
28 emission group are <0.5%, even for the 5275 GtC scenarios.

### 1 **3.3.3 Land Carbon Uptake**

2 The terrestrial biosphere takes up a relatively small fraction of the cumulative carbon  
3 emissions (3-15% of the total by the year 3000), but displays interesting dynamics (Figure 9,  
4 Panel C and Panel D).

5 Initially, global land carbon exhibits a rapid increase, driven primarily by the CO<sub>2</sub> fertilization  
6 effect. Despite much higher peak atmospheric CO<sub>2</sub> levels, peak land carbon uptake is very  
7 similar in the 2275 to 5275 GtC scenarios, indicating that there is a limit to the amount of  
8 carbon which can be taken up by the terrestrial biosphere in the UVic model.

9 After 2100 or so (earlier in the PULSE scenarios), global land carbon declines in most  
10 scenarios. The timing and magnitude of the decline is strongly dependent on the emission  
11 scenario (both in terms of total cumulative emissions and emission rate). For the 1275 GtC  
12 scenarios, the decline results in losses of about 70 to 130 GtC of land carbon between 2100  
13 and 3000. In the 2275 GtC scenarios, land carbon declines are much more modest, ranging  
14 between about 20 and 30 GtC, as carbon losses in tropical regions are approximately balanced  
15 by gains in high latitude regions.

16 To some degree in the 3375 GtC scenarios, but noticeably more so in the 4275 and 5275 GtC  
17 scenarios, ‘roller-coaster’ type behaviour is evident in land carbon, where the initial CO<sub>2</sub>  
18 fertilization driven increase of land carbon is followed by a decline, before undergoing a slow  
19 recovery towards the end of the simulation. This decline in land carbon after the peak is a  
20 result of carbon losses in the Tropics (Figure 10A) associated with temperature-driven  
21 mortality of tropical broadleaf forest (in tropical South America, SE Asia, and tropical  
22 Africa), and replacement by C4-grass and shrub. The increase in land carbon following the  
23 “dip” is driven by expansion of boreal needleleaf forest, as it displaces shrub and C3-grass  
24 tundra at high latitudes. Land carbon continues to decline in the Tropics over this time period,  
25 but is dominated by land carbon gain at high northern latitudes (Figure 10B).

26 Land carbon uptake does not show a monotonic response with increasing cumulative  
27 emissions, owing to temperature related declines at higher cumulative emissions (3275 – 5275  
28 GtC) outweighing any CO<sub>2</sub> fertilization driven increase. Despite having the highest  
29 atmospheric CO<sub>2</sub> concentration, the 5275 GtC scenarios feature the smallest absolute and  
30 fractional land carbon uptake, while the 4275 GtC scenarios have the third highest absolute  
31 uptake and the second smallest fractional uptake. Absolute uptake values increase between

1 the 1275 GtC and 2275 GtC scenarios, before declining, while fractional uptake values are  
2 highest in the 1275 GtC scenarios. This suggests that threshold behaviour may be occurring in  
3 global land carbon, driven by strong temperature related losses at higher levels of cumulative  
4 emissions (3275 – 5275 GtC).

5 Slight path dependence is evident in the 5275 GtC scenarios, with the PULSE scenario  
6 showing slightly lower land carbon uptake than the other scenarios (Figure 9C). Throughout  
7 the model integration, the PULSE scenarios shows less land carbon uptake at high latitudes  
8 and more uptake in the Tropics than its counterparts, but by the end of the model integration,  
9 the land carbon difference in the PULSE scenario originates from central Asia, where C3  
10 grass is replaced by needleleaf and shrub (not shown), which is not the case in the other  
11 scenarios.

12 The land carbon cycle response to warming and elevated atmospheric CO<sub>2</sub> levels differs  
13 widely among models (Friedlingstein et al. 2006; Arora et al. 2013; Zickfeld et al. 2013).  
14 Compared to other EMICs, land carbon uptake in the UVic ESCM is quite weak (Plattner et  
15 al. 2008; Zickfeld et al. 2013). Land carbon uptake in the UVic ESCM exhibits high  
16 sensitivities to both CO<sub>2</sub> and temperature (Eby et al. 2013), which implies a strong CO<sub>2</sub>  
17 fertilization effect, but also strong climate-carbon cycle feedbacks. Unlike previous studies,  
18 which found the land uptake fraction to remain relatively constant or decrease slightly with  
19 increasing cumulative emissions (Plattner et al. 2008; Zickfeld et al. 2013), we find the land  
20 uptake fraction to decrease substantially with increasing cumulative emissions. These  
21 previous studies, however, explored a narrower range of cumulative emissions (up to about  
22 3800 GtC in Zickfeld et al. 2013).

23 The exclusion of permafrost carbon from this study could potentially affect land carbon  
24 uptake in a future climate. MacDougall et al. (2012) utilized a modified version of the UVic  
25 ESCM with a coupled permafrost carbon model and found that permafrost soils could release  
26 between 68 GtC and 508 GtC by 2100 under the RCP 2.6 – RCP 8.5 scenarios - on the same  
27 order of magnitude as the global land carbon uptake values found in this study. The addition  
28 of permafrost carbon could turn large portions of the high latitude regions into net sources of  
29 carbon (MacDougall et al., 2012), and the added warming, in addition to fueling further  
30 carbon release from permafrost regions through feedback loops, could exacerbate the declines  
31 in land carbon exhibited by tropical regions in this study.

1 Another source of uncertainty in land carbon uptake is the coupling between the carbon and  
2 the nitrogen cycle. The land carbon cycle component of the UVic ESCM, like most land  
3 carbon cycle models, does not include a representation of the nitrogen cycle. In models that  
4 include coupled carbon and nitrogen cycles, the CO<sub>2</sub> fertilization effect under future CO<sub>2</sub>  
5 levels is reduced, since enhanced plant growth increases its need for mineralized nitrogen, and  
6 associated increases in litter inputs to the soil carbon pool can increase microbial demand for  
7 nitrogen (meaning there would be less available for plant use) (Thornton et al. 2007). This  
8 may suggest that the UVic ESCM could be overestimating the effects of CO<sub>2</sub> fertilization on  
9 land carbon uptake. Though plant and microbial nitrogen demand may increase in a warmer  
10 climate, the availability of usable nitrogen may also increase in a warmer climate (Rustad et  
11 al. 2001), which would reduce the negative effect that nitrogen limitation exerts on CO<sub>2</sub>  
12 fertilization.

13

#### 14 **4 Summary and conclusions**

15 This study explores the path dependence of the climate and carbon cycle response under CO<sub>2</sub>  
16 scenarios spanning a broad range of cumulative emissions and emission rates. We use the  
17 UVic Earth System Model of intermediate complexity, which is forced with 24 CO<sub>2</sub> emission  
18 scenarios across five cumulative emission groups (1275, 2275, 3275, 4275 and 5275 GtC).  
19 Each cumulative emission group includes a variety of peak and decline scenarios with  
20 differing emission rates, an overshoot scenario, and an instantaneous pulse scenario.

21 Our results indicate that the century-scale global mean temperature response after cessation of  
22 CO<sub>2</sub> emissions is independent of emission pathway and proportional to cumulative emissions,  
23 consistent with the findings of previous studies (Eby et al. 2009; Zickfeld et al. 2009; Zickfeld  
24 et al. 2012; Nohara et al. 2013).

25 The ratio of global mean temperature change to cumulative emissions – referred to as the  
26 Transient Climate Response to Cumulative Emissions (TCRE) – is found to be constant for  
27 cumulative emissions lower than ~1500 GtC, but to decline with higher cumulative emissions.  
28 The TCRE is also found to decrease with increasing peak emission rate, in contrast to the  
29 results from another study (Krasting et al. 2014).

30 The century-scale thermosteric sea level rise is also found to be approximately independent of  
31 emission pathway. Small differences in sea level rise between scenarios within the same

1 cumulative emission group at the end of the simulation arise from the sluggish response of the  
2 ocean to radiative forcing.

3 Similarly to global mean temperature and thermosteric sea level rise, we find the long-term  
4 response of Arctic September sea ice cover to be independent of emission pathway and  
5 determined only by cumulative emissions. The long-term sea ice cover declines with  
6 increasing cumulative emissions, with a critical cumulative emission level for the loss of year-  
7 round Arctic sea ice found to be between 1275 and 2275 GtC. Changes in Arctic September  
8 sea ice cover also show an approximately proportional relationship with cumulative  
9 emissions, with the change in sea ice cover per unit change in cumulative emissions differing  
10 slightly across scenarios and cumulative emission groups.

11 The peak response of the Atlantic meridional overturning circulation (AMOC) is found to be  
12 path dependent, with pathways featuring higher emission rates yielding the largest AMOC  
13 decline. Eventually, however, the AMOC responses converge, and there is little difference in  
14 the year-3000 AMOC strength across scenarios within a cumulative emission group. At no  
15 point does the AMOC shutdown in any of the 24 scenarios, suggesting that either the AMOC  
16 in the UVic ESCM does not exhibit multiple stable states, or that the critical transition point  
17 was not reached.

18 Similarly to the physical climate variables, the century-scale carbon cycle response after  
19 cessation of emissions is found to be approximately independent of emission pathway. Small  
20 differences in year-3000 ocean carbon uptake between scenarios at high cumulative emission  
21 levels arise from the slow response of the ocean to changes in atmospheric CO<sub>2</sub> and  
22 temperature. We also find a small difference in year-3000 land carbon uptake between  
23 scenarios at high cumulative emissions (5275 GtC) due to hysteresis in regional land cover  
24 changes.

25 The year-3000 land carbon uptake exhibits a non-monotonic response to cumulative CO<sub>2</sub>  
26 emissions, with land carbon uptake increasing for cumulative emissions up to 2275 GtC and  
27 then decreasing. This indicates that for cumulative emissions greater than 2275 GtC, land  
28 carbon gains associated with the CO<sub>2</sub> fertilization effect are more than offset by warming  
29 related losses. Expressed as a fraction of cumulative emissions, land carbon uptake at year  
30 3000 is largest for the 1275 GtC scenarios (15%) and declines with increasing cumulative  
31 emissions, to just 3% for the 5275 GtC scenarios.



1 Ocean carbon uptake at year 3000 increases in absolute terms with increasing cumulative  
2 emissions, as a function of increasing atmospheric CO<sub>2</sub> levels at higher cumulative emissions.  
3 The fraction of cumulative CO<sub>2</sub> emissions taken up by the ocean at the year 3000 decreases  
4 with increasing cumulative emissions, from 56% in the 1275 GtC scenarios to 35% in the  
5 5275 GtC scenarios. As a result of reduced fractional land and carbon uptake with increasing  
6 cumulative emissions, the year-3000 airborne fraction of CO<sub>2</sub> increases with increasing  
7 cumulative emissions, from 29% in the 1275 GtC scenarios to 63% in the 5275 GtC  
8 scenarios.

9 In summary, this study shows that the long-term climate and carbon cycle response is  
10 approximately independent of emission pathway over a broad range of cumulative emissions.  
11 This study also confirms the approximately proportional relationship between global warming  
12 and cumulative carbon emissions. The TCRE deviates from constancy for cumulative  
13 emissions greater than ~1500 GtC and is sensitive to the rate of emissions, but these path  
14 dependencies are a smaller source of uncertainty in the TCRE than inter-model differences.

15

#### 16 **Author Contributions**

17 K. Zickfeld conceived the study, T. Herrington and K. Zickfeld designed the model  
18 experiments, T. Herrington performed the model simulations and analyzed the data, T.  
19 Herrington and K. Zickfeld interpreted the data and wrote the manuscript.

20

#### 21 **Acknowledgements**

22 K. Zickfeld acknowledges support from the National Science and Engineering Research  
23 Council (NSERC) CREATE and Discovery Grant Programs.

24

## 1 **References**

- 2 Allen M, Frame D, Huntingford C, Jones CD, Lowe JA, Meinshausen M, Meinshausen N  
3 (2009) Greenhouse-gas emission targets for limiting global warming to 2°C. *Nature* 458:  
4 1163-1166.  
5
- 6 Archer D (1996) A data-driven model of the global calcite lysocline. *Global Biogeochem.*  
7 *Cycles* 10: 511-526.  
8
- 9 Arora VK, Boer GJ, Friedlingstein P, Eby M, Jones CD, Christian JR, Bonan G, Bopp L,  
10 Brovkin V, Cadule P, Hajima T, Ilyina T, Lindsay K, Tjiputra JF, Wu T (2013). Carbon-  
11 Concentration and Carbon-Climate Feedbacks in CMIP5 Earth System Models. *J. Clim.* 26:  
12 5289-5314.  
13
- 14 Boden TA, Marland G, Andres RJ (2012) Carbon Dioxide Information Analysis Center, Oak  
15 Ridge National Laboratory, U.S. Department of Energy, Oak Ridge, Tenn., U.S.A.  
16 [http://cdiac.ornl.gov/trends/emis/tre\\_glob\\_2009.html](http://cdiac.ornl.gov/trends/emis/tre_glob_2009.html). Accessed: September 30 2012.  
17
- 18 Bouttes N, Gregory JM, Lowe JA (2013) The Reversibility of Sea Level Rise. *J. Clim.* 26:  
19 2502-2513.  
20
- 21 Comiso JC (2012) Large decadal decline of the Arctic multiyear ice cover. *J. Clim.* 25: 1176-  
22 1193.  
23
- 24 Eby M, Zickfeld K, Montenegro A, Archer D, Meissner K, Weaver A (2009) Lifetime of  
25 anthropogenic climate change: millennial time scales of potential CO<sub>2</sub> and surface  
26 temperature perturbations. *J. Clim.* 22: 2501-2511.  
27
- 28 England MH, Gupta AS, Pitman AJ (2009) Constraining future greenhouse gas emissions by  
29 a cumulative target. *Proceedings of the National Academy of Sciences* 106: 16539-16540.  
30

1 Friedlingstein P, Cox P, Betts R, Bopp L, Von Bloh W, Brovkin V, Cadule P, Doney S, Eby  
2 M, Fung I (2006) Climate-carbon cycle feedback analysis: Results from the C4MIP model  
3 intercomparison. *J. Clim.* 19: 3337-3353.  
4

5 Frölicher TL, Joos F (2010) Reversible and irreversible impacts of greenhouse gas emissions  
6 in multi-century projections with the NCAR global coupled carbon cycle-climate model.  
7 *Climate Dyn.* 35:1439-1459.  
8

9 Frölicher TL, Winton M, Sarmiento JL (2014) Continued global warming after CO2  
10 emissions stoppage. *Nature Clim. Change* 4: 40-44.  
11

12 Gent PR and McWilliams JC (1990) Isopycnal mixing in ocean circulation models. *J. Phys.*  
13 *Oceanogr.* 20: 150-155.  
14

15 Gillett NP, Arora VK, Zickfeld K, Marshall SJ, Merryfield WJ (2011) Ongoing climate  
16 change following a complete cessation of carbon dioxide emissions. *Nature Geoscience* 4: 83-  
17 87.  
18

19 Gillett NP, Arora VK, Matthews HD, Allen MR (2013) Constraining the ratio of global  
20 warming to cumulative CO2 emissions using CMIP5 simulations. *J. Clim.* 26:6844-6858.  
21

22 Houghton RA (2008) Carbon Dioxide Information Analysis Center, Oak Ridge National  
23 Laboratory, U.S. Department of Energy, Oak Ridge, Tenn., U.S.A.  
24 <http://cdiac.ornl.gov/trends/landuse/houghton/houghton.html>. September 30 2012.  
25

26 Krasting JP, Dunne JP, Shevliakova E, Stoufer RJ (2014) Trajectory sensitivity of the  
27 transient climate response to cumulative carbon emissions. *Geophys. Res. Lett.* 41: 2520-  
28 2527.  
29

30 Lowe JA, Huntingford C, Raper SCB, Jones CD, Liddicoat SK, Gohar LK (2009) How  
31 difficult is it to recover from dangerous levels of global warming? *Environ. Res. Lett.*  
32 4:014012.  
33

1 MacDougall AH, Avis CA, Weaver AJ (2012) Significant contribution to climate warming  
2 from the permafrost carbon feedback. *Nature Geoscience* 5: 719-721.  
3  
4 MacDougall AH (2014), A modelling study of the permafrost carbon cycle feedback to  
5 climate change: feedback strength, timing, and carbon cycle consequences, PhD thesis,  
6 University of Victoria, BC, Canada, 118 p.  
7  
8 Matthews H D and Caldeira K (2008) Stabilizing climate requires near-zero emissions  
9 *Geophys. Res. Lett.* 35: L04705.  
10  
11 Matthews HD, Gillett NP, Stott PA, Zickfeld K (2009) The proportionality of global warming  
12 to cumulative carbon emissions. *Nature* 459: 829-832.  
13  
14 Meissner K, Weaver A, Matthews H, Cox P (2003) The role of land surface dynamics in  
15 glacial inception: A study with the UVic Earth System Model. *Clim. Dyn.* 21: 515-537.  
16  
17 Meinshausen M., et al. (2009) Greenhouse-gas emission targets for limiting global warming  
18 to 2 °C. *Nature* 458: 1158–1162.  
19  
20 Messner D, Schellnhuber J, Rahmstorf S, Klingensfeld D (2010) The budget approach: A  
21 framework for a global transformation toward a low-carbon economy. *Journal of Renewable*  
22 *and Sustainable Energy* 2: 1-14.  
23  
24 Nohara D, Yoshida Y, Misumi K, Ohba M (2013) Dependency of climate change and carbon  
25 cycle on CO<sub>2</sub> emission pathways. *Environmental Research Letters* 8: 014047.  
26  
27 Plattner G, Knutti R, Joos F, Stocker T, Von Bloh W, Brovkin V, Cameron D, Driesschaert E,  
28 Dutkiewicz S, Eby M (2008) Long-term climate commitments projected with climate-carbon  
29 cycle models. *J. Clim.* 21: 2721-2751.  
30  
31 Rahmstorf S (2000) The thermohaline ocean circulation: A system with dangerous  
32 thresholds? *Clim. Change* 46: 247-256.  
33

1 Rustad L, Campbell J, Marion G, Norby R, Mitchell M, Hartley A, Cornelissen J, Gurevitch J  
2 (2001) A meta-analysis of the response of soil respiration, net nitrogen mineralization, and  
3 aboveground plant growth to experimental ecosystem warming. *Oecologia* 126: 543-562.  
4

5 Schmittner A, Oschlies A, Giraud X, Eby M, Simmons H (2005) A global model of the  
6 marine ecosystem for long-term simulations: Sensitivity to ocean mixing, buoyancy forcing,  
7 particle sinking, and dissolved organic matter cycling. *Global Biogeochem. Cycles* 19:  
8 GB3004.  
9

10 Send U, Lankhorst M, Kanzow T (2011) Observation of decadal change in the Atlantic  
11 meridional overturning circulation using 10 years of continuous transport data. *Geophys. Res.*  
12 *Lett.* 38: L24606.  
13

14 Solomon S, Plattner G, Knutti R, Friedlingstein P (2009) Irreversible climate change due to  
15 carbon dioxide emissions. *Proceedings of the National Academy of Sciences* 106: 1704-1709.  
16

17 Solomon, S., Qin, D., Manning, M.: *Climate Change 2007: The Physical Science Basis*,  
18 Working Group I Contribution to the Fourth Assessment Report of the Intergovernmental  
19 Panel on Climate Change, Cambridge University Press, Cambridge, UK, 2007.  
20

21 Stroeve J, Holland MM, Meier W, Scambos T, Serreze M (2007) Arctic sea ice decline:  
22 Faster than forecast. *Geophys. Res. Lett.* 34: L09501.  
23

24 Thornton PE, Lamarque J, Rosenbloom NA, Mahowald NM (2007) Influence of  
25 carbon-nitrogen cycle coupling on land model response to CO<sub>2</sub> fertilization and climate  
26 variability. *Global Biogeochem. Cycles* 21: GB4018.  
27

28 Weaver AJ, Eby M, Wiebe EC, Bitz CM, Duffy PB, Ewen TL, Fanning AF, Holland MM,  
29 MacFadyen A, Matthews HD (2001) The UVic Earth System Climate Model: Model  
30 description, climatology, and applications to past, present and future climates. *Atmosphere-*  
31 *Ocean* 39: 361-428.  
32

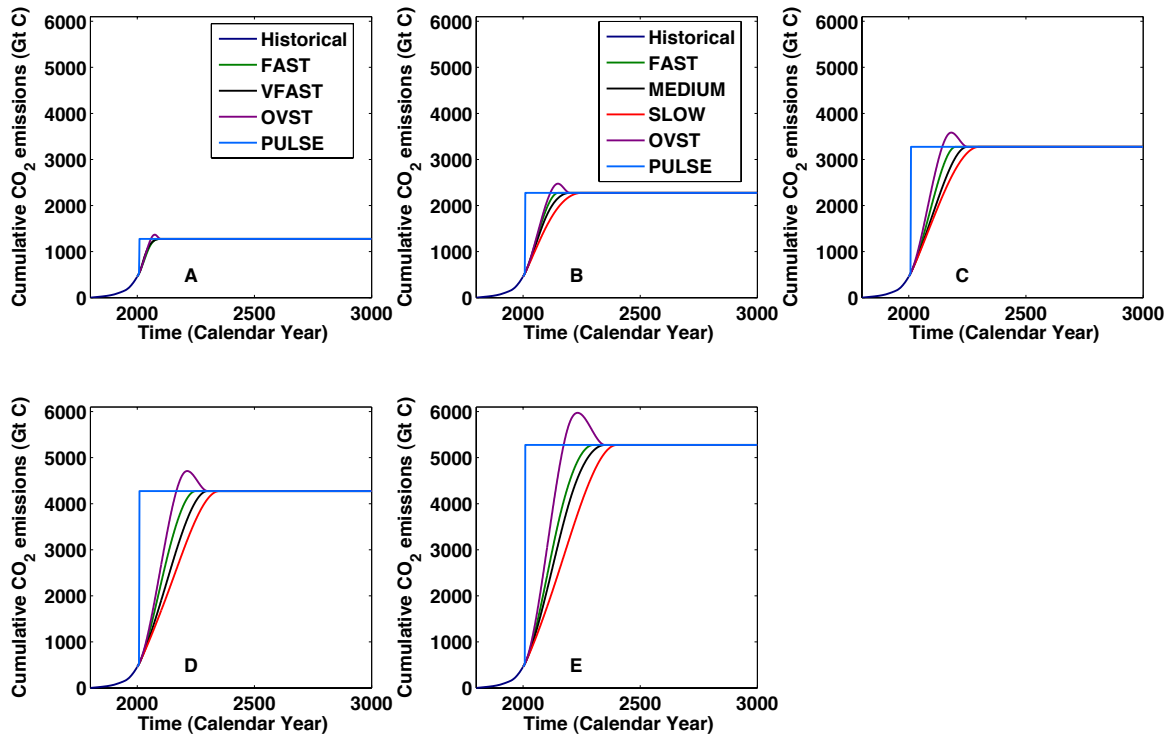
- 1 Wullschleger S, Tschaplinski T, Norby R (2002) Plant water relations at elevated CO<sub>2</sub>–  
2 implications for water-limited environments. *Plant, Cell Environ.* 25: 319-331.  
3
- 4 Zickfeld K, Eby M, Matthews HD, Weaver AJ (2009) Setting cumulative emissions targets to  
5 reduce the risk of dangerous climate change. *Proceedings of the National Academy of*  
6 *Sciences* 106: 16129-16134.  
7
- 8 Zickfeld K, Arora VK, Gillett NP (2012) Is the climate response to CO<sub>2</sub> emissions path  
9 dependent? *Geophys. Res. Lett.* 39: L05703.  
10
- 11 Zickfeld K, Eby M, Alexander K, Weaver AJ et al. (2013) Long-term climate change  
12 commitment and reversibility: An EMIC intercomparison, *J. Clim.* 26: 5782-5809.  
13

1 Table 1. The 24 emission scenarios and their characteristics. Emissions include both fossil  
 2 fuel and land-use change emissions. Cumulative emissions are from year 1800 onward.

Cumulative Emissions	Scenario	Maximum Emission Rate (GtC yr <sup>-1</sup> )	Year of Emission Cessation
1275 GtC	FAST	14.1	2100
	VFAST	17.4	2100
	OVST	16.9	2100
	PULSE	376.7	2010
2275 GtC	FAST	17.1	2100
	MEDIUM	14.9	2100
	SLOW	11.5	2250
	OVST	18.7	2100
	PULSE	883.5	2010
3275 GtC	FAST	19.1	2200
	MEDIUM	14.7	2250
	SLOW	12.9	2300
	OVST	24.2	2250
	PULSE	1390.4	2010
4275 GtC	FAST	22	2250
	MEDIUM	17	2300
	SLOW	14.1	2350
	OVST	28.2	2300
	PULSE	1897.2	2010
5275 GtC	FAST	24.9	2300
	MEDIUM	21.1	2350
	SLOW	15.9	2400
	OVST	34.9	2350
	PULSE	2404.1	2010

3

4



1

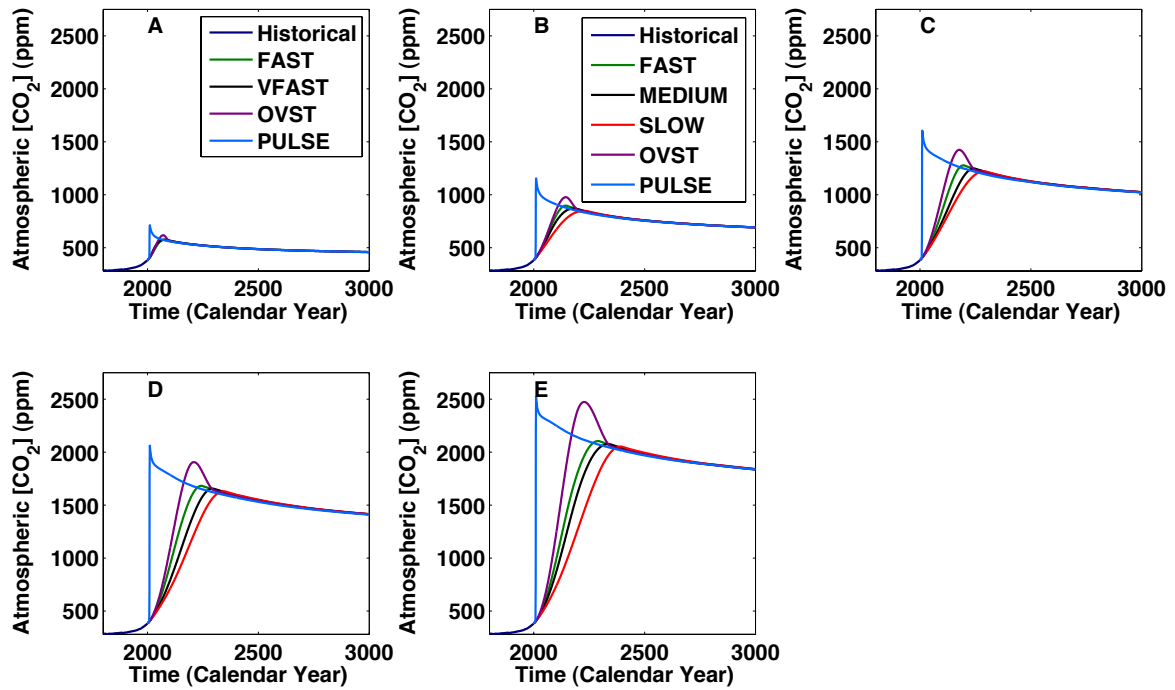
2 Figure 1. Global cumulative CO<sub>2</sub> emissions (fossil fuel plus LUC emissions) for the 1275 –  
 3 5275 GtC cumulative emission scenarios. A) 1275 GtC scenarios, B) 2275 GtC scenarios, C)  
 4 3275 GtC scenarios, D) 4275 GtC scenarios, and E) 5275 GtC scenarios. (Note: legend for B  
 5 also applies to C, D, and E).

6

7

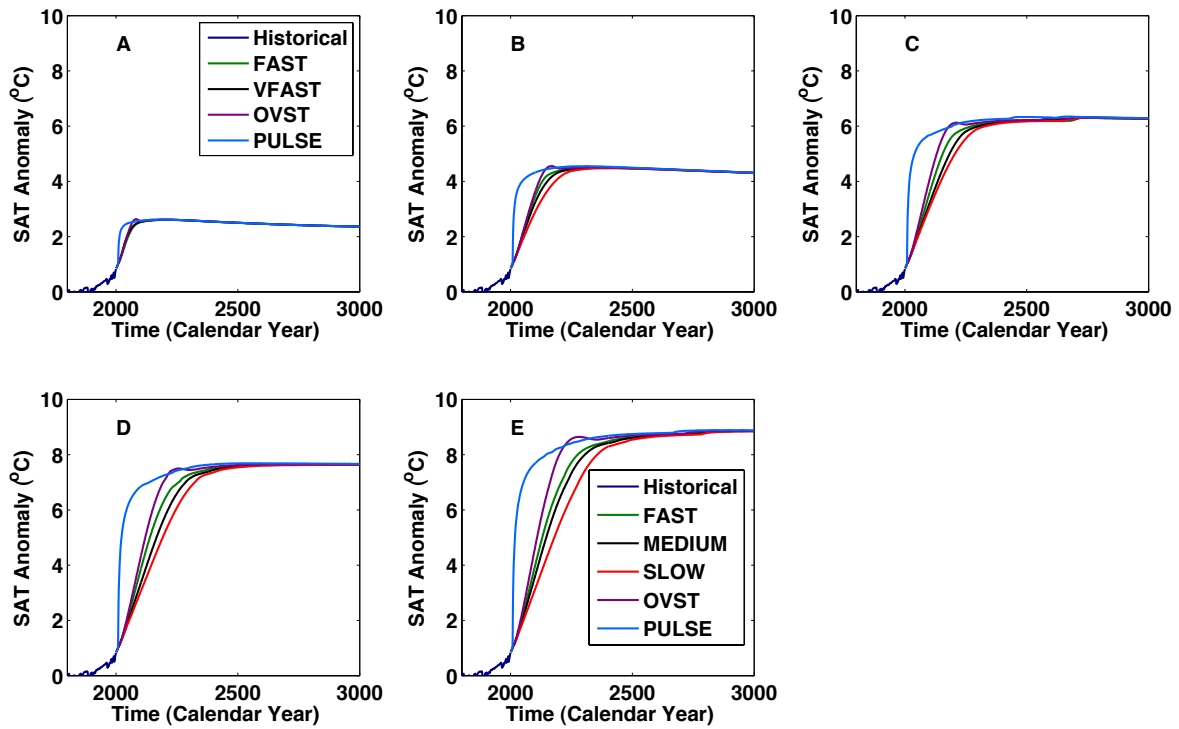
8





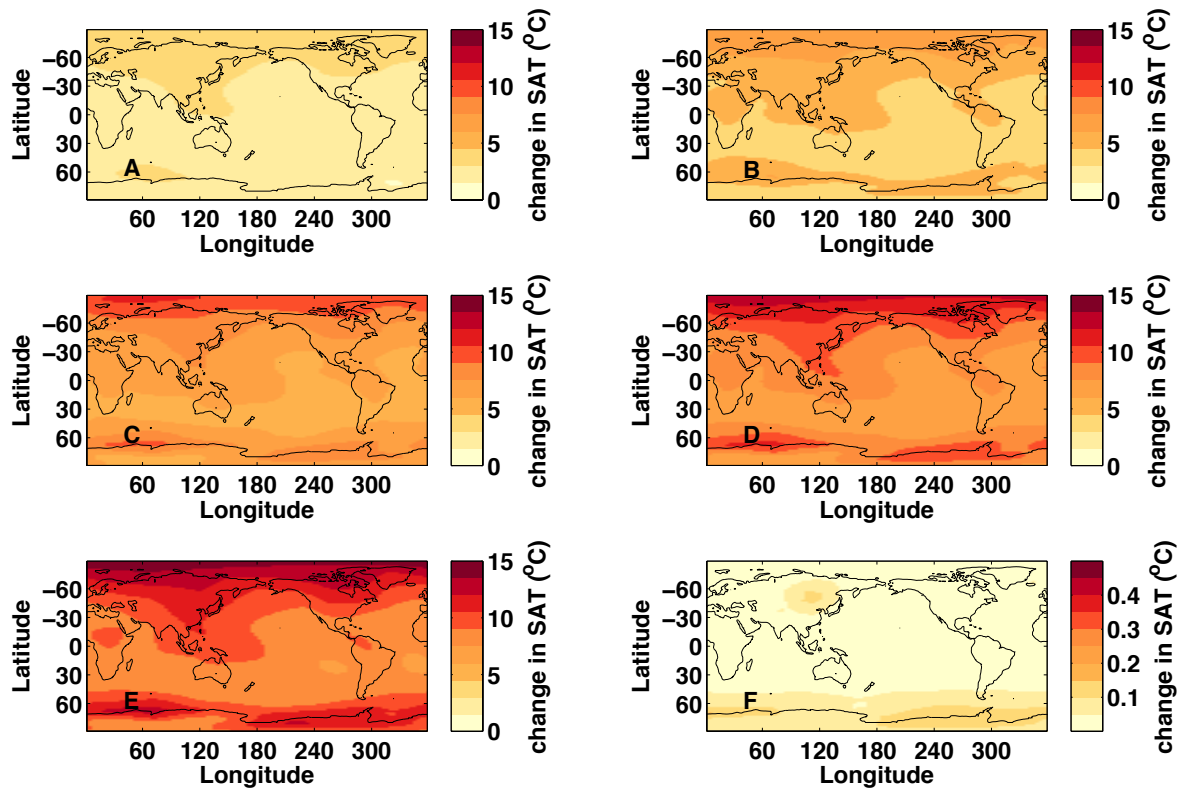
1  
2  
3  
4  
5

Figure 2. Atmospheric CO<sub>2</sub> concentration for the 1275 – 5275 GtC scenarios. A) 1275 GtC scenarios, B) 2275 GtC scenarios, C) 3275 GtC scenarios, D) 4275 GtC scenarios, and E) 5275 GtC scenarios. (Note: legend for B also applies to C, D, and E).



1  
 2 Figure 3. Global mean surface air temperature (SAT) anomaly relative to the year 1800 for  
 3 the 1275 – 5275 GtC scenarios. A) 1275 GtC scenarios, B) 2275 GtC scenarios, C) 3275 GtC  
 4 scenarios, D) 4275 GtC scenarios, and E) 5275 GtC scenarios. (Note: legend for E also  
 5 applies to B, C, and D).

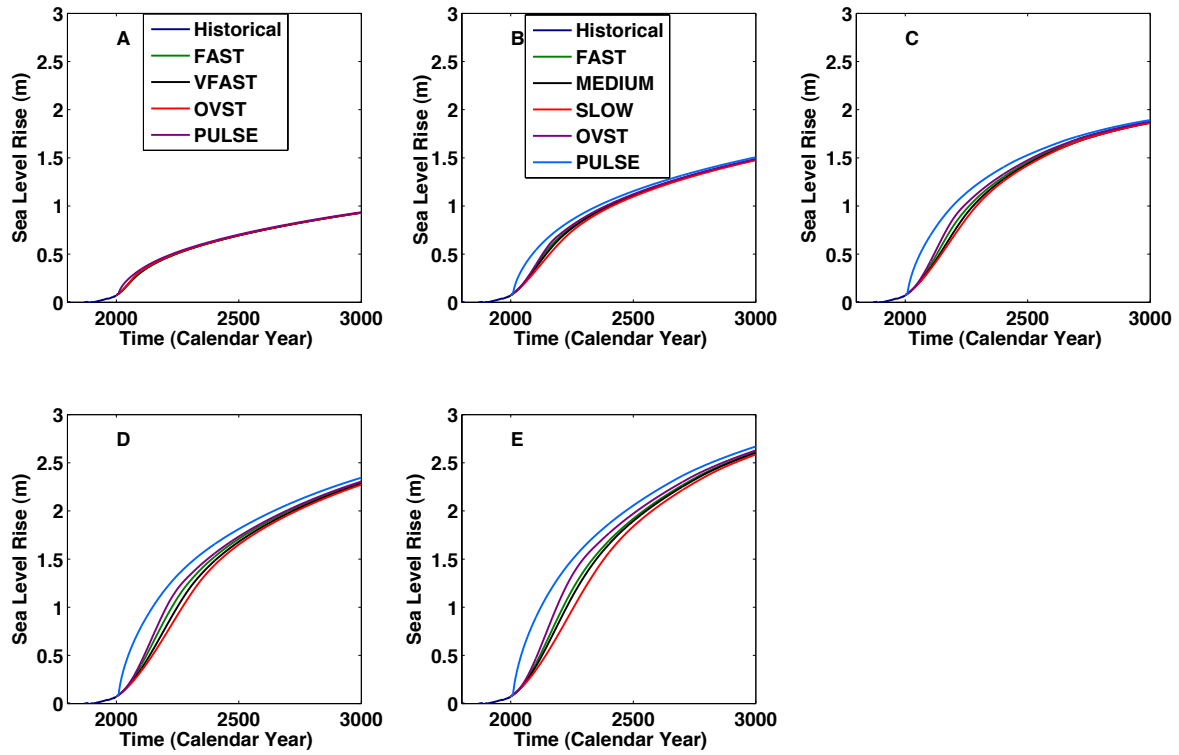
6



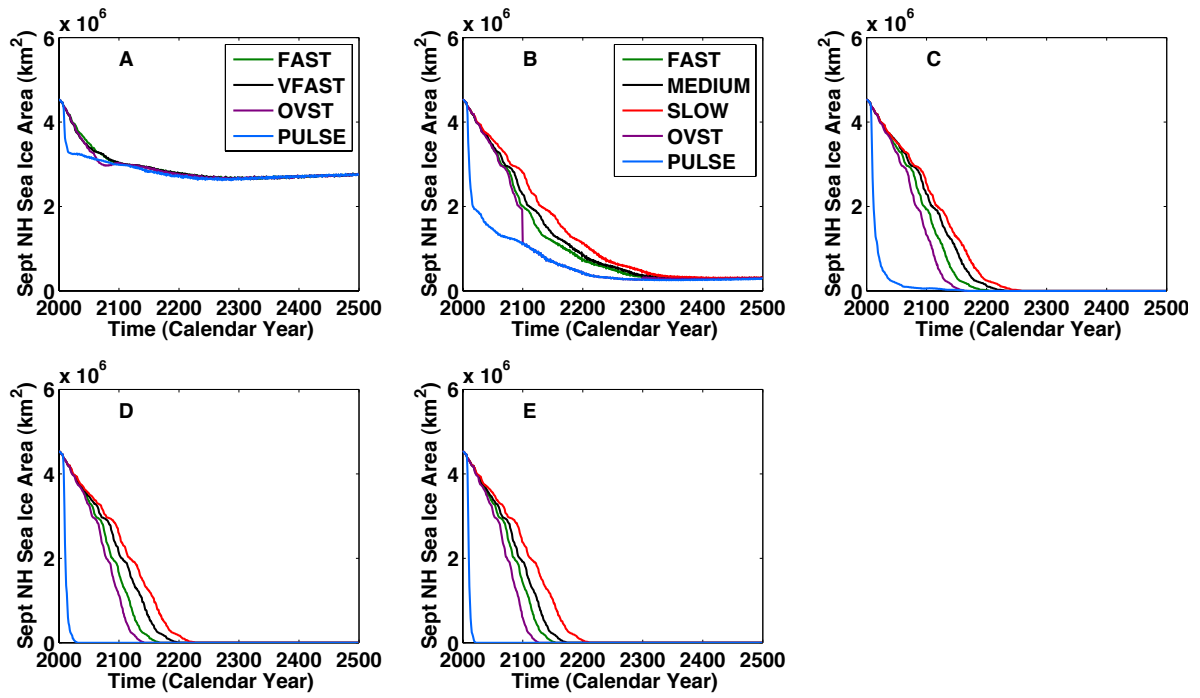
1

2 Figure 4. Year 3000 surface air temperature (SAT) anomalies relative to 1800 for select  
 3 scenarios. A) 1275 GtC FAST, B) 2275 GtC FAST, C) 3275 GtC FAST, D) 4275 GtC FAST,  
 4 E) 5275 GtC FAST, and F) 5275 GtC PULSE minus SLOW. Note that the color scale for F is  
 5 different from that for the other panels.

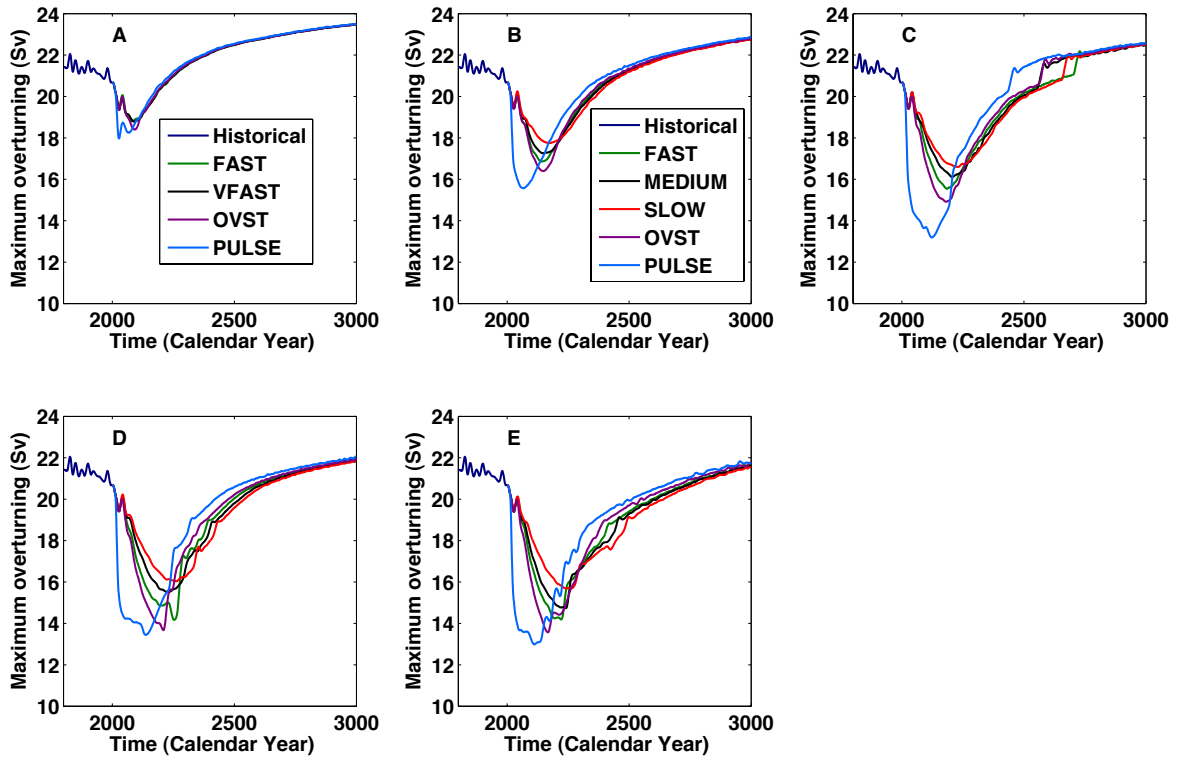
6



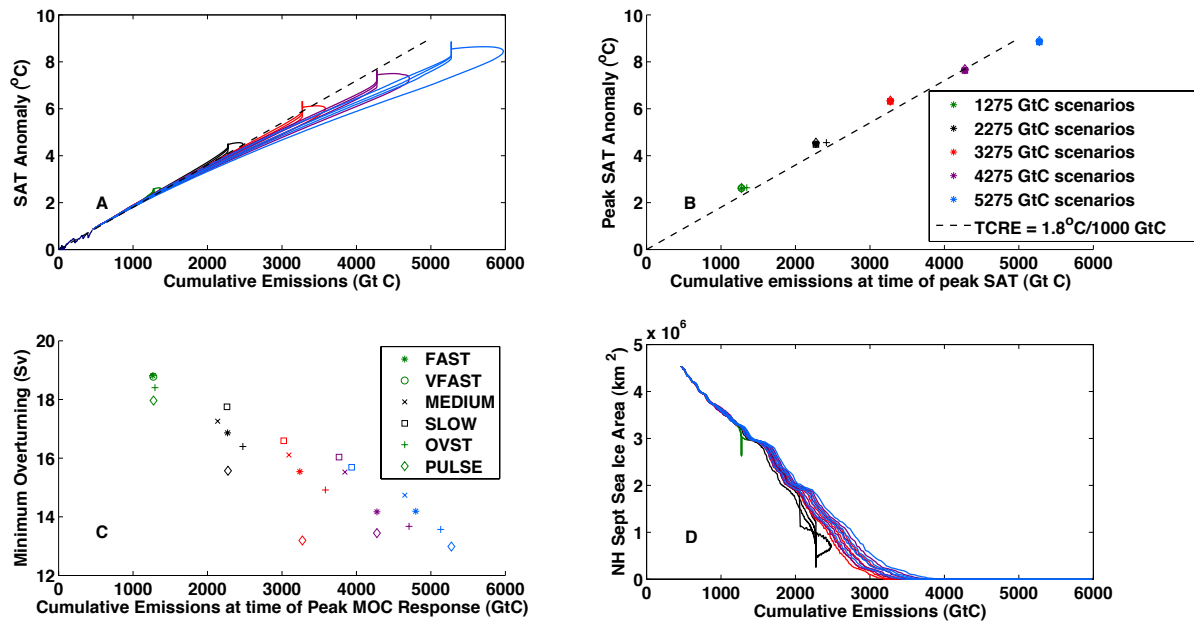
1  
 2 Figure 5. Global mean thermosteric sea level rise (relative to 1800) for the 1275 - 5275 GtC  
 3 scenarios. A) 1275 GtC scenarios, B) 2275 GtC scenarios, C) 3275 GtC scenarios, D) 4275  
 4 GtC scenarios, and E) 5275 GtC scenarios. (Note: legend for B also applies to C, D, and E).  
 5



1  
 2 Figure 6. September Northern Hemisphere (NH) sea ice area ( $\text{km}^2$ ) for the 1275 – 5275 GtC  
 3 scenarios. A) 1275 GtC scenarios, B) 2275 GtC scenarios, C) 3275 GtC scenarios, D) 4275  
 4 GtC scenarios, and E) 5275 GtC scenarios. (Note: legend for B also applies to C, D, and E).  
 5

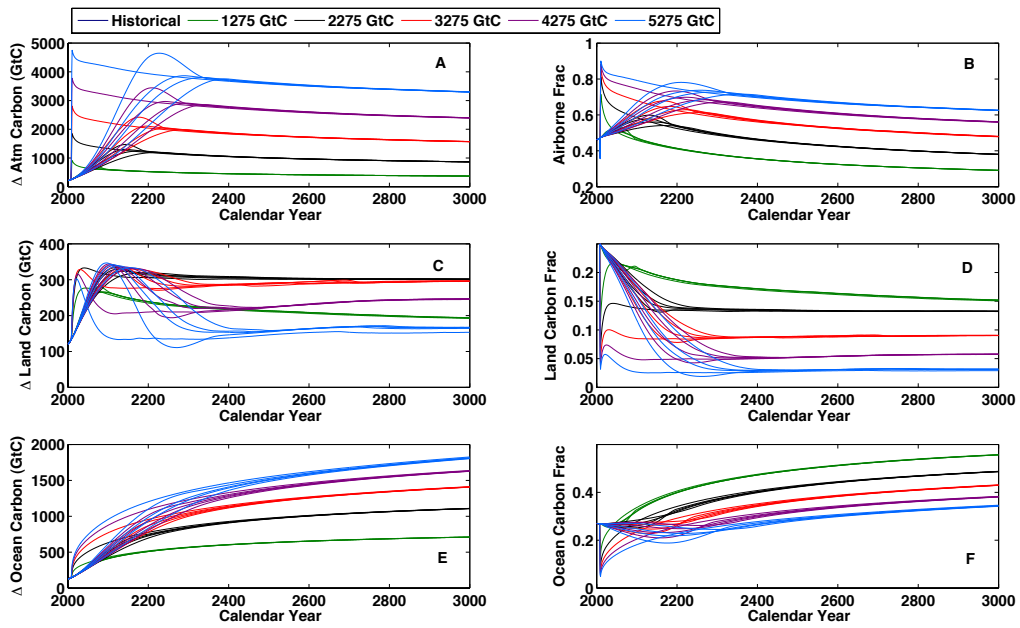


1  
2 Figure 7. Atlantic Meridional Overturning Circulation (AMOC) index (defined as the  
3 maximum overturning streamfunction) for the 1275 - 5275 GtC scenarios. A) 1275 GtC  
4 scenarios, B) 2275 GtC scenarios, C) 3275 GtC scenarios, D) 4275 GtC scenarios, and E)  
5 5275 GtC scenarios. (Note: legend for B also applies to C, D, and E)  
6



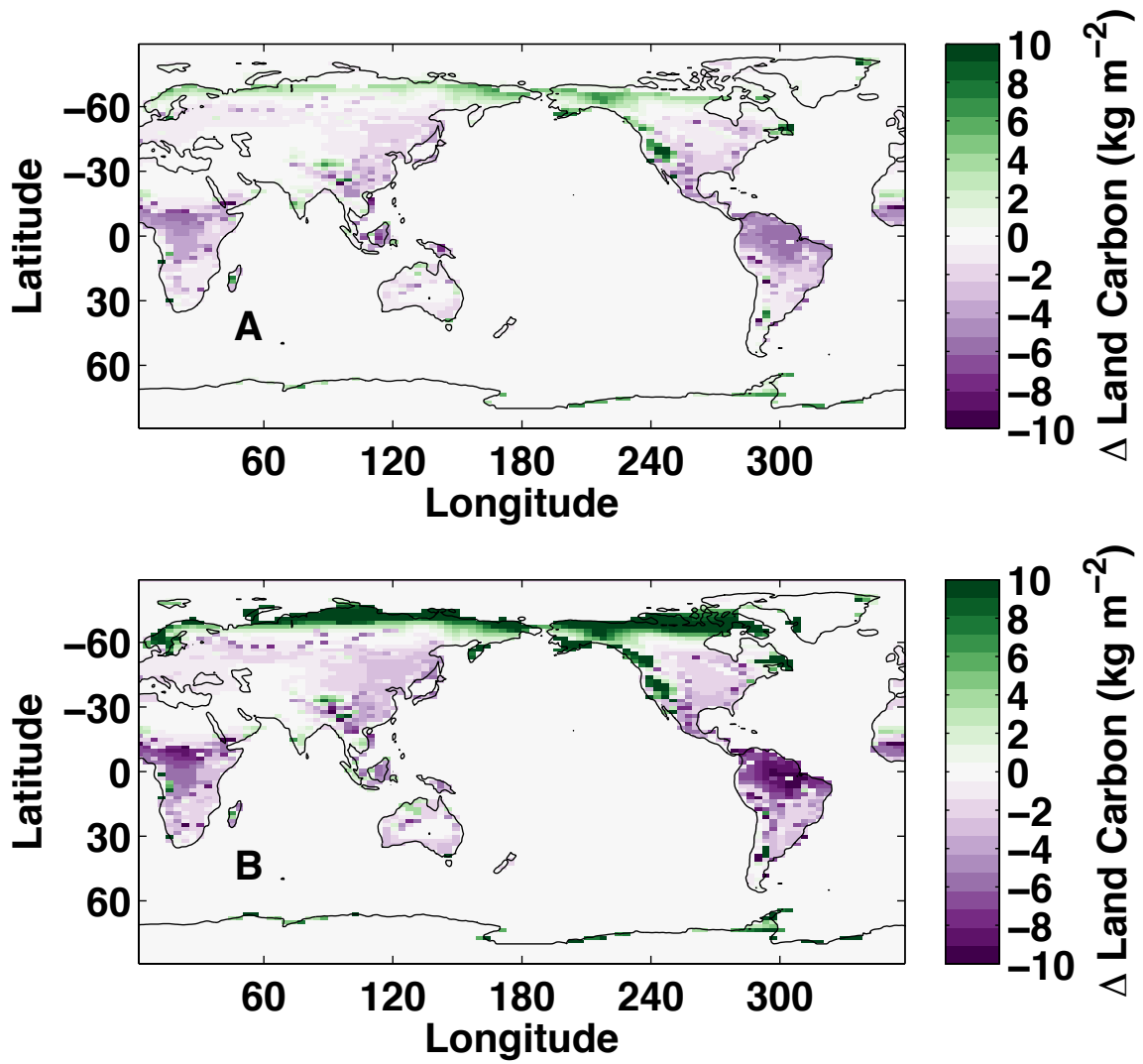
1  
 2 Figure 8. Relationship between physical climate variables and cumulative carbon emissions.  
 3 A) Global mean surface air temperature (SAT) anomaly (relative to 1800), B) Peak global  
 4 mean surface air temperature anomaly (relative to 1800), C) Minimum overturning  
 5 circulation, and D) September Northern Hemisphere (NH) sea ice area. The dashed line in  
 6 panels A and B shows the relationship between SAT change and cumulative emissions using  
 7 the average TCRE computed at the time of CO<sub>2</sub> doubling (1.8°C TtC<sup>-1</sup>). Note: The colour  
 8 legend in B applies to all panels and the symbol legend in C applies to panels B and C.

9  
 10



1  
 2 Figure 9. Global carbon cycle response. A) Atmospheric carbon anomaly (w.r.t. 1800), B)  
 3 Airborne fraction of cumulative emissions, C) Land carbon anomaly (w.r.t. 1800), D)  
 4 Fraction of cumulative emissions taken up by the land, E) Ocean carbon anomaly (w.r.t.  
 5 1800), F) Ocean uptake fraction. Note that vertical axes vary.





1  
 2 Figure 10. Changes in land carbon for the 5275 GtC FAST scenario. A) Minimum (year  
 3 2310) minus peak (year 2170) total land carbon, B) Year 2990 minus minimum (year 2310)  
 4 total land carbon.

5